

# Phase-Charge Duality of a Josephson junction in a fluctuating electromagnetic environment

S. Corlevi<sup>1</sup>, W. Guichard<sup>1,2</sup>, F.W.J. Hekking<sup>2</sup>, and D.B. Haviland<sup>1</sup>

<sup>1</sup>*Nanostructure Physics, Royal Institute of Technology,  
10691 Stockholm, Sweden*

<sup>2</sup>*University Joseph Fourier and CNRS,  
B.P. 166, 25 Avenue des Martyrs,  
38042 Grenoble-cedex 09, France*

We have measured the current-voltage characteristics of a single Josephson junction placed in a high impedance environment. The transfer of Cooper pairs through the junction is governed by overdamped quasicharge dynamics, leading to Coulomb blockade and Bloch oscillations. Exact duality exists to the standard overdamped phase dynamics of a Josephson junction, resulting in a dual shape of the current-voltage characteristic, with current and voltage changing roles. We demonstrate this duality with experiments which allow for a quantitative comparison with a theory that includes the effect of fluctuations due to finite temperature of the electromagnetic environment.

PACS numbers: 73.23.Hk, 73.40.Gk, 74.50.+r

Duality often plays a central role in our understanding of the physical world. Some physical models, for example the harmonic oscillator, contain the remarkable property of self duality, where we can map the model back onto itself in such a way that the role of physically conjugate degrees of freedom is interchanged. Another generic model which exhibits self duality is that of a quantum particle in a cosine potential coupled to an ohmic heat-bath [1]. This model also describes the electrodynamics of a circuit consisting of a single Josephson junction shunted by a resistor [2]. In this Letter we present an experimental verification of this self duality.

In the standard theory of the Josephson effect [3, 4], a current  $I$  which is less than the critical current  $I_C$  flows with zero voltage difference across the tunnel junction, corresponding to a static state where the phase difference across the junction has no time dependence. This region of the current-voltage characteristic, known as supercurrent branch, is well-separated from the dissipative quasiparticle branch by a voltage of twice the superconducting gap  $V = 2\Delta/e$ . However, since early work by Ivanchenko and Zil'berman [5], it is known that in the presence of an impedance  $Z_{\text{env}}(\omega)$  close to a Josephson junction with small capacitance  $C$ , phase diffusion will occur, and therefore dissipative behavior exists also for the supercurrent with finite, time averaged voltages  $\langle V \rangle$  below the gap. The resulting DC current-voltage characteristic (IVC) of the junction consists of a supercurrent peak, with a tail at finite voltages originating from the Josephson oscillations at the frequency  $f_J = 2e\langle V \rangle/h$ . The detailed IVC of the tunnel junction depends on the charging energy  $E_C = e^2/2C$ , the Josephson coupling energy  $E_J = \hbar I_C/2e$ , and the impedance of the environment  $Z_{\text{env}}(\omega)$ . When the impedance is frequency independent  $\Re[Z_{\text{env}}] = R$ , phase diffusion occurs if  $Q = \pi(R/R_Q)\sqrt{E_J/2E_C} \ll 1$ , where  $R_Q = h/4e^2 = 6.45 \text{ k}\Omega$  is the quantum resistance. This limit, usually referred

to as overdamped phase dynamics, was analyzed in [5], where the IVC of the junction was calculated in the presence of thermal fluctuations due to Nyquist noise in the resistor. Although this analytic result had been known for quite some time, the supercurrent peak was only recently measured for a small-capacitance Josephson junction embedded in a carefully designed low impedance environment, where  $R \ll R_Q$  for all frequencies [6].

The picture developed in [5] and experimentally verified in [6] is based on the classical, non-linear phase dynamics of the junction and is valid in a low impedance environment. When  $R \simeq R_Q$  quantum fluctuations of the phase become important and a theoretical description of incoherent tunneling of individual Cooper pairs can be applied to calculate the junction IVC for an arbitrary  $Z_{\text{env}}$  when  $E_J \ll E_C$  [7]. This theory predicts that the supercurrent peak moves to higher voltages, opening a Coulomb gap in the IVC of the junction.

Of great interest however is the case when  $E_J \geq E_C$  and  $R \gg R_Q$ , usually referred to as the underdamped case ( $Q \gg 1$ ), where the incoherent tunneling picture breaks down. Here a situation exactly dual to the above-mentioned classical overdamped phase dynamics occurs. Based on duality arguments [8] and a quantitative theory in terms of Bloch bands [9, 10], the IVC of the junction was predicted to show a voltage peak near zero current corresponding to Coulomb blockade, and a tail at finite currents corresponding to Bloch oscillations with frequency  $f_B = \langle I \rangle/2e$ . During each period of the oscillations exactly one Cooper pair tunnels through the junction. In this picture the junction circuit is described by the classical, non-linear dynamics of the quasicharge, which is the conjugate variable to the Josephson phase. In view of duality, when the phase dynamics is underdamped the corresponding quasicharge dynamics is overdamped. The quasicharge then evolves in time according to the Langevin equation  $dq/dt = (I_b + \delta I) - V/R$ . Here,  $I_b$  is the bias current and  $\delta I$  a random noise component

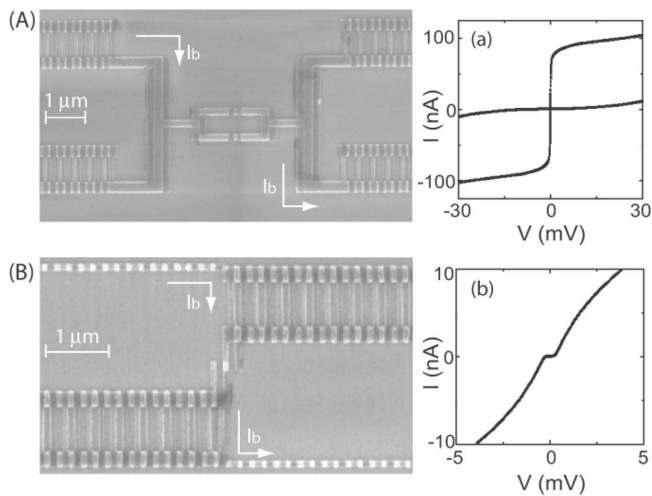


FIG. 1: (A) and (B): SEM images of the SQUID and single junction sample configuration. A symmetric bias  $I_b$  is applied from the top-left array to the bottom-right array. (a) and (b): IVC of the current bias lines for the two configurations. (a) from top to bottom: two SQUID arrays in series in the superconducting ( $R_0 \approx 50 \text{ k}\Omega$ ) and insulating ( $R_0 \approx 50 \text{ M}\Omega$ ) case. (b): two non-SQUID arrays in series ( $R_0 \approx 10 \text{ M}\Omega$ ).

induced by the resistance; the voltage across the junction  $V = dE_0(q)/dq$  is given by the derivative of the lowest Bloch energy band (see inset of Fig. 2). The IVC of a single junction can be analytically calculated from the Langevin equation for the quasicharge [9, 10, 11].

Few experiments have probed a single Josephson junction in the regime  $R \gg R_Q$  due to difficulties in designing an environment with such high impedance at the frequency  $f_B$  ( $\approx 10^{10} \text{ Hz}$ ). Small on-chip resistors [12, 13] and two-dimensional electron gas beneath the junction [14] have been used to achieve a high impedance environment. In our experiment, Josephson junction SQUID arrays are used to bias the junction. The advantage of the SQUID configuration is that the effective impedance of the environment can be tuned *in situ* by applying a magnetic field perpendicular to the SQUID loops. Although no systematic characterization of the arrays impedance at frequencies of the order of  $f_B$  has been performed, they have been successfully employed [15] to demonstrate how the environment induces Coulomb blockade and Bloch oscillations in a single Josephson junction in the weak coupling regime  $E_J < E_C$ .

In this paper we present experimental results on single junctions where  $\Re[Z_{\text{env}}] \gg R_Q$ . We have studied a single junction with SQUID geometry (Fig. 1A), which allows for a systematic study of the IVC of the same single junction as it is tuned from strong ( $E_J > E_C$ ) to weak coupling ( $E_J < E_C$ ), with the magnetic field. We also studied a single non-tunable junction (Fig. 1B) with strong coupling, where the exact dual of the overdamped Josephson effect is realized. Here we make for the first time a detailed quantitative comparison with theory.

The Al/AlO<sub>x</sub>/Al tunnel junctions are fabricated by double angle evaporation through a mask patterned by electron beam lithography. The samples are mounted in a RF-tight copper box and measured in a dilution refrigerator with base temperature of 15 mK. No special cold microwave filters were implemented in the cryostat, as the arrays themselves are acting as extremely good filters, protecting the CPT from fluctuations generated in the bias circuit. The single junctions are biased by four Josephson junction arrays and the IVC is measured in a four point configuration. One pair of arrays is used to apply a symmetric bias; the current is measured directly with a current preamplifier (modified Stanford Research System SR570). The voltage across the single junction is measured through the other pair of arrays with a high input impedance differential amplifier having an input current of 3 fA (Burr-Brown INA116). Since the impedance of the voltage leads can be in the G $\Omega$  range, even such small input current can lead to voltages comparable with the blockade voltage of the single junction, making the measurement of the voltage over the junction impossible.

In the sample layout presented in Fig. 1A, the single junction has a SQUID geometry, and it is biased by four SQUID arrays. Each array consists of 60 SQUIDs with a nominal area of  $0.06 \mu\text{m}^2$ . Each junction of the central SQUID has an area of  $\approx 0.02 \mu\text{m}^2$ . The loop of the single junction SQUID is designed to be 10 times larger than the loop area of the SQUID arrays, enabling a periodic modulation of the  $E_J/E_C$  of the single SQUID which is incommensurate with the period of modulation of the environment impedance. As the magnetic field is increased, the SQUID arrays undergo a superconducting-insulator quantum phase transition [16]. This results in an increase of the zero bias resistance  $R_0$  of the arrays over several orders of magnitude (from k $\Omega$  up to G $\Omega$ ). Figure 1a shows the IVC of the two biasing SQUID arrays at magnetic fields corresponding to the maximum and minimum value of  $R_0$ .

Figure 2 shows the IVC of the single junction SQUID at two different values of magnetic field. The field values were chosen so that the zero bias resistance of the biasing leads was the same for both curves ( $R_0 \approx 10 \text{ M}\Omega$ ). However, the  $E_J/E_C$  ratio of the single junction SQUID is different for the two curves. Curve A in Fig. 2 corresponds to the maximum value of the Josephson coupling, while in curve B the Josephson coupling was at a minimum. We estimate the values of  $E_J/E_C$  for the two curves from the samples parameters. The charging energy  $E_C = e^2/2C = 45 \mu\text{eV}$  is calculated from the junction area, which gives a capacitance  $C \approx 1.8 \text{ fF}$  assuming a specific capacitance of  $45 \text{ fF}/\mu\text{m}^2$ .  $E_J$  of the single junction SQUID depends on the magnetic field  $B$ , and it can be expressed as  $E_J = R_Q \Delta / 2R_N |\cos(\pi B/B_0)|$ , where  $R_N = 2.8 \text{ k}\Omega$  is the normal state resistance of the SQUID,  $\Delta \approx 200 \mu\text{eV}$  the superconducting gap of Al, and  $B_0 = 16 \text{ G}$  the measured period of the SQUID modulation. Here we assume that the two junctions in the SQUID are identical. Thus we calculate

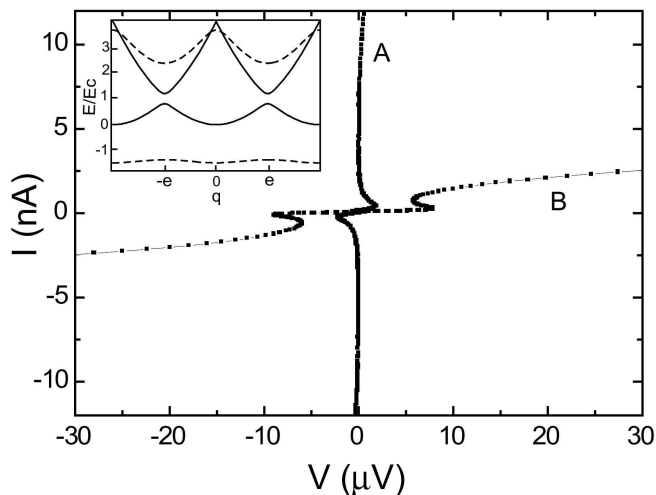


FIG. 2: IVC of a single junction SQUID at two different values of magnetic field, corresponding to (A)  $E_J/E_C = 4.5$  and (B)  $E_J/E_C \leq 0.2$ . At these values the biasing SQUID arrays had the same zero bias resistance  $R_0 \approx 10$  M $\Omega$ . The inset shows the two lowest energy bands of a single junction calculated for  $E_J/E_C = 2$  (dashed line) and  $E_J/E_C = 0.2$  (solid line).

$E_J/E_C = 4.5$  at the maximum (curve A). Experimental uncertainties make determination much less accurate at the minimum of the SQUID modulation, where we estimate  $E_J/E_C \leq 0.2$  (curve B).

Both curves A and B in Fig. 2 show a Coulomb blockade feature, followed by a back bending region due to the Bloch oscillations. The differences between these two curves are qualitatively understood from the Bloch band theory [10, 17]. The critical voltage, or maximum blockade voltage, is determined by the shape of the lowest energy band,  $V_C = \max[dE_0(q)/dq]$ . For  $E_J/E_C > 1$  the lowest energy band becomes very flat (see inset of Fig. 2), which explains why curve A has a smaller blockade voltage than curve B. Furthermore, the gap between the lowest and first excited energy band strongly depends on  $E_J/E_C$  (inset Fig. 2). The gap determines the maximum current, or Zener break-down current  $I_Z$ , above which Zener tunneling to higher bands leads to dissipation and increased voltage across the junction. For  $E_J/E_C = 4.5$  the experiment shows  $I_Z \simeq 10$  nA, whereas for  $E_J/E_C \leq 0.2$ , we measure  $I_Z \simeq 0.5$  nA, in qualitative agreement with theory.

This qualitative comparison can be made more quantitative if we take in to account the effect of fluctuations due to the finite temperature electromagnetic environment, which cause the measured blockade voltage to be smaller than the theoretical critical voltage  $V_C$ . Using duality arguments, Beloborodov *et al.* [11] have calculated the IVC of a junction in a high impedance environment with  $E_J/E_C > 1$  in the presence of thermal fluctuations. In the theory the environment consists of a resistor ( $Z_{\text{env}} = R$ ) characterized by gaussian noise with temperature  $T_{\text{noise}}$ . Ref. [11] assumes the noise to be white, *i.e.*, to have classical correlations, which is the

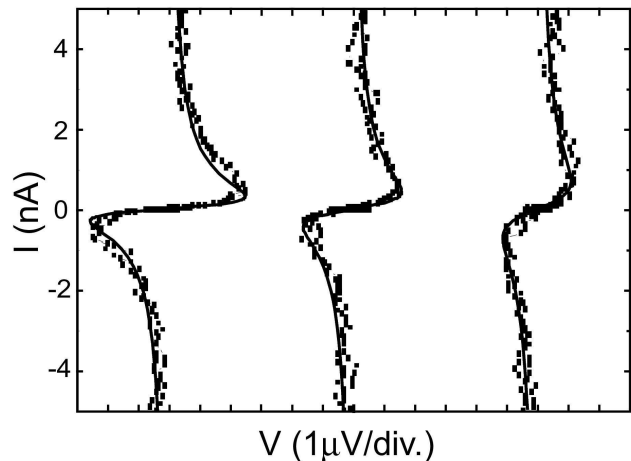


FIG. 3: IVC of a single junction in the overdamped quasicharge regime at different temperature (points) and the theoretical prediction (solid lines). In the fit  $V_C = 30$   $\mu$ V. From left to right the cryostat (fitting noise) temperatures are: T=50 mK (160 mK), 250 mK (260 mK), 300 mK (400 mK).

case as long as  $k_B T_{\text{noise}} > R_Q e V_C / R$ . For our experiment, this condition is satisfied as long as  $T_{\text{noise}} > 5$  mK.

In the experiment, the biasing arrays may generate more complicated fluctuations, but for the purpose of comparison we describe the arrays by one parameter,  $R$ , which represents the most basic way to characterize their fluctuations. For a bias current less than  $I_Z$ , the IVC of the junction obtained in [11] can be expressed in a form dual to that of [5, 6]

$$\langle V \rangle = V_C \Im \left[ \frac{I_{1-i\beta e I_b R / \pi}(\beta e V_C / \pi)}{I_{-i\beta e I_b R / \pi}(\beta e V_C / \pi)} \right], \quad (1)$$

where  $\beta = 1/k_B T_{\text{noise}}$  is the inverse of the noise temperature and  $I_\nu(z)$  is the modified Bessel function of argument  $z$  and complex order  $\nu$ .

We have experimentally studied the influence of the cryostat temperature on the IVC of samples with the layout presented in Fig. 1B. Here the single junction under test (area  $\approx 0.02$   $\mu\text{m}^2$ ) is not tunable, and it is current biased by two non-SQUID arrays consisting of 16 junctions with nominal area  $0.01$   $\mu\text{m}^2$ . The IVC of these arrays (Fig. 1b) shows a strong Coulomb blockade, providing a good current bias for the single junction. However the voltage probes are SQUID arrays, allowing the tunability of their impedance to an optimal value. We have found that the tunability of the voltage probes is essential for this type of experiment.

In Fig. 3 the measured IVCs at fixed magnetic field ( $B = 262$  G) and various temperatures are shown together with the theoretical curves calculated using Eq. (1). For these samples, the Josephson coupling of the single junction was large enough to realize the exact dual of the overdamped Josephson effect. In contrast to previous works [15], we were able to measure

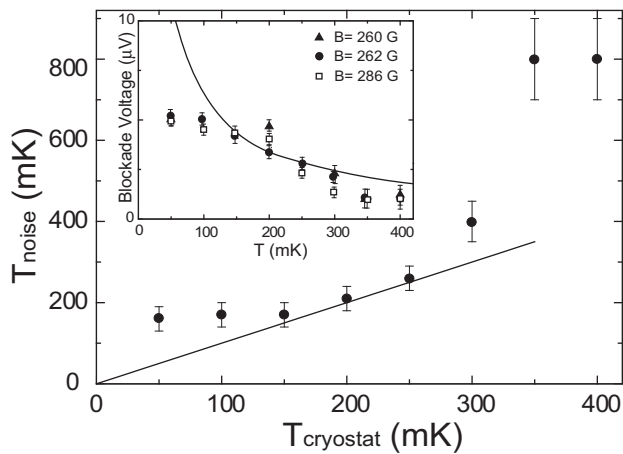


FIG. 4: Noise temperature as determined from fitting to theory (Fig. 3) plotted vs. the cryostat temperature. Inset: Measured blockade voltage for three sets of data (symbols) and calculated blockade voltage for  $V_C = 30 \mu\text{V}$  (solid line) if  $T_{\text{noise}} = T_{\text{cryostat}} = T$ .

IVCs showing a complete back bending to a zero voltage current, allowing for the first time a quantitative comparison between the theory and experiment. Excellent agreement is achieved using one value of the parameter  $R = 150 \text{ k}\Omega$  for all curves, while adjusting the noise temperature  $T_{\text{noise}}$  for a best fit. For the theoretical curves the value  $V_C = 30 \mu\text{V}$  was used, which compares very well to the estimated critical voltage  $V_C = 28 \pm 7 \mu\text{V}$ . This value was calculated [18] from the energies  $E_J = 270 \mu\text{eV}$  and  $E_C \approx 90 \mu\text{eV}$ , determined from the junction parameters as previously described ( $R_N = 2 \text{ k}\Omega$ ,  $C \approx 0.9 \text{ fF}$ ). The value  $R = 150 \text{ k}\Omega$ , which represents the theoretical effective frequency independent impedance seen by the single junction, compares rather well with the measured  $R_0 \approx 200 \text{ k}\Omega$  of the voltage probes (SQUID arrays) at the particular magnetic field studied. These arrays exhibit a weaker Coulomb blockade than the non-SQUID arrays, hence the former determine the impedance which the junction sees.

Figure 4 shows a comparison between  $T_{\text{cryostat}}$  and  $T_{\text{noise}}$ , where the latter is determined by the fit to theory as shown in Fig. 3. In the region 175 mK to 250 mK, the two temperatures coincide, but the noise tempera-

ture does not go below 175 mK. This saturation indicates the existence of residual noise with an effective temperature around 175 mK in the measurement system. As reported in [6], excess noise may be a consequence of inadequate filtering of the measurement leads. Another possible source of excess noise is shot noise in the current biasing arrays. These arrays have a strong Coulomb blockade, where charge transport is discrete and a shot noise is expected. We also find excess noise when the cryostat is above 250 mK. This temperature is close to the estimated odd-even free energy difference [19] for the islands in the arrays, above which quasiparticle tunneling in the arrays would lead to excess noise.

Thus we see that noise reduces the measured blockade voltage below the theoretically predicted maximum critical voltage  $V_C = 30 \mu\text{V}$ . To further illustrate this point we plot the measured blockade voltage vs.  $T_{\text{cryostat}}$  in the inset of Fig. 4. The solid line is the theoretical prediction if  $T_{\text{cryostat}} = T_{\text{noise}}$ , independent of the parameter  $R$ . We see that a blockade voltage of the order of  $10 \mu\text{V}$  would be expected at a temperature of 50 mK, if the excess noise could be reduced. It is remarkable that this theory, which uses a minimal description of the fluctuations in the Josephson junction arrays, gives the correct order of magnitude for  $V_C(T)$ , and very accurately reproduces the shape of the IVC. A more complex model, including frequency dependent impedance of the arrays, as well as additional sources of noise may give better correspondence, but at the price of many more parameters.

In summary, we have experimentally studied the IVC of a single Josephson junction in a high impedance environment ( $R > R_Q$ ) in the strong coupling regime ( $E_J > E_C$ ), where the dual of the classical Josephson effect is realized. We show qualitative agreement with the Bloch band theory for the same single junction as the ratio  $E_J/E_C$  is tuned with the magnetic field. By taking in to account the finite temperature of the electromagnetic environment, we can quantitatively explain the measured data with a minimal theory, where gaussian fluctuations are described by one parameter.

We acknowledge discussions with H. Grabert, G. Ingold, and M.H. Devoret. This work was partially supported by the Swedish SSF Center NanoDev, the EU project SQUBIT and Institut Universitaire de France.

[1] U. Weiss, *Quantum dissipative systems* (World Scientific Publishing, 1999).  
[2] The heat bath of the original model corresponds to a reflectionless transmission line. If the line parameters are chosen appropriately, it is equivalent to a resistor.  
[3] B. D. Josephson, *Phys. Lett.* **1**, 251 (1962).  
[4] K. K. Likharev, *Dynamics of Josephson junctions and circuits* (Gordon and Breach Science Publisher, 1986).  
[5] Y. M. Ivanchenko and L. A. Zilberman, *Sov. Phys. JETP* **28**, 1272 (1969).

[6] A. Steinbach, P. Joyez, A. Cottet, D. Esteve, M. H. Devoret, M. E. Huber, and J. M. Martinis, *Phys. Rev. Lett.* **87**, 137003 (2001).  
[7] G. L. Ingold and Y. V. Nazarov, in *Single Charge Tunneling*, edited by H. Grabert and M. H. Devoret (Plenum, New York, 1991), Chap. 2.  
[8] A. Widom, G. Megaloudis, T. D. Clark, and R. J. Prance, *J. Phys. A* **15**, 1561 (1982).  
[9] D. V. Averin, A. B. Zorin, and K. K. Likharev, *Sov. Phys. JETP* **61**, 407 (1985).

- [10] K. K. Likharev and A. B. Zorin, *J. Low Temp. Phys* **59**, 347 (1985).
- [11] I. S. Beloborodov, F. W. J. Hekking, and F. Pistolesi, in *New directions in Mesoscopic Physics (Towards Nanoscience)*, edited by R. Fazio, V. F. Gantmakher, and Y. Imry (Kluwer Academic Publisher, 2002), p. 339, cond-mat/0304102.
- [12] L. S. Kuzmin, Y. V. Nazarov, D. B. Haviland, P. Delsing, and T. Claeson, *Phys. Rev. Lett.* **67**, 1161 (1991).
- [13] S. V. Lotkhov, S. A. Bogoslovsky, A. B. Zorin, and J. Niemeyer, *Phys. Rev. Lett.* **91**, 197002 (2003).
- [14] J. Kycia, J. Chen, R. Therrien, Ç. Kurdak, K. Campman, A. Gossard, and J. Clarke, *Phys. Rev. Lett.* **87**, 017002 (2001).
- [15] M. Watanabe and D. B. Haviland, *Phys. Rev. Lett.* **86**, 5120 (2001); *Phys. Rev. B* **67**, 094505 (2003).
- [16] K. B. Efetov, *Sov. Phys. JETP* **51**, 1015 (1980).
- [17] G. Schön and A. D. Zaikin, *Phys. Rep.* **198**, 237 (1990).
- [18] A. B. Zorin, private communication.
- [19] M. Tuominen, J. Hergenrother, T. Tighe, and M. Tinkham, *Phys. Rev. Lett.* **69**, 1997 (1992).